MASSIVE GALAXIES IN COSMOS: EVOLUTION OF BLACK HOLE VERSUS BULGE MASS BUT NOT VERSUS TOTAL STELLAR MASS OVER THE LAST 9 Gyr?[*]

KNUD JAHNKE[1], ANGELA BONGIORNO[2,3], MARCELLA BRUSA[2], PETER CAPAK[4], NICO CAPPELLUTI[2], MAURICIO CISTERNAS[1], FRANCESCA CIVANO[5], JAMES COLBERT[4], ANDREA COMASTRI[6], MARTIN ELVIS[5], GÜNTHER HASINGER[7], OLIVIER ILBERT[8], CHRIS IMPEY[9], KATHERINE INSKIP[1], ANTON M. KOEKEMOER[10], SIMON LILLY[11], CHRISTIAN MAIER[11], ANDREA MERLONI[2,12], DOMINIK RIECHERS[4,14], MARA SALVATO[4,7], EVA SCHINNERER[1], NICK Z. SCOVILLE[4], JOHN SILVERMAN[11], YOSHI TANIGUCHI[13], JONATHAN R. TRUMP[9], AND LIN YAN[4]

[1] Max-Planck-Institut für Astronomie, Königstuhl 17, D-69117 Heidelberg, Germany; jahnke@mpia.de
[2] Max-Planck-Institut für Extraterrestrische Physik, Giessenbachstrasse, D-85741 Garching b. München, Germany
[3] University of Maryland, Baltimore County, 1000 Hilltop Circle, Baltimore, MD 21250, USA
[4] California Institute of Technology, 1200 East California Boulevard, MC 249-17, Pasadena, CA 91125, USA
[5] Harvard Smithsonian Center for Astrophysics, 60 Garden Street, Cambridge, MA 02138, USA
[6] INAF-Osservatorio Astronomico di Bologna, via Ranzani 1, I-40127 Bologna, Italy
[7] Max-Planck-Institut für Plasmaphysik, Boltzmannstrasse 2, D-85741 Garching, Germany
[8] Institute for Astronomy, 2680 Woodlawn Drive, University of Hawaii, Honolulu, HI 96822, USA
[9] Steward Observatory, University of Arizona, 933 North Cherry Avenue, Tucson, AZ 85721, USA
[10] Space Telescope Science Institute, 3700 San Martin Drive, Baltimore, MD 21218, USA
[11] Department of Physics, ETH Zürich, CH-8093 Zürich, Switzerland
[12] Excellence Cluster Universe, TUM, Boltzmannstr. 2, D-85748 Garching, Germany
[13] Research Center for Space and Cosmic Evolution, Ehime University, Bunkyo-cho, Matsuyama 790-8577, Japan

ABSTRACT

We constrain the ratio of black hole (BH) mass to total stellar mass of type-1 active galactic nuclei (AGNs) in the COSMOS survey at $1 < z < 2$. For 10 AGNs at mean redshift $z \sim 1.4$ with both *Hubble Space Telescope* (*HST*)/ACS and *HST*/NICMOS imaging data, we are able to compute the total stellar mass $M_{*,\mathrm{total}}$, based on rest-frame UV-to-optical host galaxy colors which constrain mass-to-light ratios. All objects have virial M_{BH} estimates available from the COSMOS Magellan/IMACS and zCOSMOS surveys. We find within errors zero difference between the $M_{\mathrm{BH}}-M_{*,\mathrm{total}}$ relation at $z \sim 1.4$ and the $M_{\mathrm{BH}}-M_{*,\mathrm{bulge}}$ relation in the local universe. Our interpretation is (1) if our objects were purely bulge-dominated, the $M_{\mathrm{BH}}-M_{*,\mathrm{bulge}}$ relation has not evolved since $z \sim 1.4$. However, (2) since we have evidence for substantial disk components, the bulges of massive galaxies ($M_{*,\mathrm{total}} = 11.1 \pm 0.3$ or $\log M_{\mathrm{BH}} \sim 8.3 \pm 0.2$) must have grown over the last 9 Gyr predominantly by redistribution of the disk into the bulge mass. Since all necessary stellar mass exists in galaxies at $z = 1.4$, no star formation or addition of external stellar material is required, but only a redistribution, e.g., induced by minor and major merging or through disk instabilities. Merging, in addition to redistributing mass in the galaxy, will add both BH and stellar/bulge mass, but does not change the overall final $M_{\mathrm{BH}}/M_{*,\mathrm{bulge}}$ ratio. Since the overall cosmic stellar and BH mass buildup trace each other tightly over time, our scenario of bulge formation in massive galaxies is *independent* of any strong BH feedback and means that the mechanism coupling BH and bulge mass until the present is very indirect.

Key words: galaxies: active – galaxies: evolution – galaxies: fundamental parameters – galaxies: nuclei

1. INTRODUCTION

Masses of galactic bulges and their central black holes (BHs) follow a tight relation in the local universe (e.g., Marconi & Hunt 2003; Häring & Rix 2004) with only 0.3 dex scatter—strong evidence for a coupled formation and evolution of galaxies and BHs. The source of this coupling is unclear, but feedback mechanisms have been proposed involving the central potential well depth regulating BH accretion, or more violent feedback from active galactic nuclei (AGNs) into their host galaxies (e.g., Hopkins et al. 2006; Somerville et al. 2008; Menci et al. 2008). While these scenarios potentially provide

ingredients for acquiring consensus with observations, all such models include ad hoc assumptions and do not work from first principles. Empirical constraints are urgently needed to investigate the actual physical processes involved in the coupled evolution.

One strong constraint is the evolution of the $M_{\mathrm{BH}}-M_{*,\mathrm{bulge}}$ relation over time. While circumstantial evidence that the value of $M_{\mathrm{BH}}/M_{*,\mathrm{bulge}}$ was larger at earlier cosmic times grows (Peng et al. 2006a, 2006b; Treu et al. 2007; Woo et al. 2008; Walter et al. 2004; Riechers et al. 2008a, 2008b, 2009), studies are subject to biases (Lauer et al. 2007) and better statistics are required to investigate where in M_{BH}, or when in cosmic time, a turnoff from the local $M_{\mathrm{BH}}-M_{*,\mathrm{bulge}}$ relation occurs.

Broad-line AGNs and their host galaxies are the only systems at higher redshifts in which both the mass of the galaxy or its bulge as well as its central BH can be estimated. Here we set constraints on an evolving $M_{\mathrm{BH}}-M_{*,\mathrm{bulge}}$ relation by computing optical color-based stellar masses (from *Hubble Space Telescope* (*HST*)/ACS and *HST*/NICMOS) and combine them with virial M_{BH} (from Magellan/IMACS and zCOSMOS/

Table 1
Sample Summary

XMM-Newton Name[a]	XID[a]	z	M_{BH}[b] $(M_\odot)$	Ref[c]	$F814W_{host}$ (AB mag)	$F160W_{host}$ (AB mag)	Sérsic n[d] $F160W$	$(B-V)_{host}^{rest}$ (Vega Mag)	$\log(M_{*,total})$[e] $(M_\odot)$
XMMU J100118.5+022739	14	1.065	8.52	1	20.70	19.41	1.9	0.38	11.18
XMMU J100046.8+020016	59	1.923	8.72	2	⋯	20.28	0.6	0.15–0.75	11.07–12.12
XMMU J095927.7+020010	219	1.248	8.07	2	22.55	20.61	2.1	0.49	11.00
XMMU J100035.3+024303	281	1.177	8.25	1, 2	22.63	20.25	3.5	0.74	11.44
XMMU J095928.5+015934	329	1.166	8.05	1, 2	22.95	21.03	1.7	0.58	10.90
XMMU J100130.7+021147	2148	1.526	8.43	1	23.45	21.15	1.5	0.40	10.88
XMMU J100243.8+020502	2261	1.260	8.05	1	⋯	21.38	⋯	0.15–0.75	10.25–11.09
XMMU J100226.9+015938	2637	1.630	8.35	1	24.12	20.72	1.8	0.73	11.64
XMMU J095903.2+022001	5049	1.131	8.40	2	22.66	20.82	1.5	0.57	10.93
XMMU J095908.1+024310	5230	1.359	8.22	1	⋯	19.13	⋯	0.15–0.75	11.21–12.08

Notes.
[a] Original *XMM-Newton* source name and ID (Cappelluti et al. 2009).
[b] Mean value where two measurements are available.
[c] Source for M_{BH}: (1) Magellan/IMACS (Trump et al. 2009b); (2) zCOSMOS/VIMOS (Merloni et al. 2009); M_{BH} errors are quoted as 0.4 dex and 0.3 dex, respectively.
[d] From free-n fit before fixing.
[e] Total uncertainty is ±0.4 dex (Section 3.3).

VLT/VIMOS) for 10 AGNs in the redshift interval $1.06 < z < 1.92$, 3.2–5.5 Gyr after the big bang.

Throughout we use AB zero-points unless otherwise noted and a cosmology of $H_0 = 70\,\mathrm{km\,s^{-1}\,Mpc^{-1}}$, $\Omega_M = 0.3$, and $\Omega_\Lambda = 0.7$.

2. DATABASE

In order to control selection effects on M_*, M_{BH} or any special relation between these two, we require a transparent sample definition. Our selection of type-1 AGNs is based on X-ray detection in the XMM-COSMOS survey (Hasinger et al. 2007; Cappelluti et al. 2009) and subsequent identification of their optical counterparts (Brusa et al. 2007). Classification as type-1 AGNs for this study uses both spectroscopic identification of broad emission lines in the Magellan/IMACS (Trump et al. 2009a) and zCOSMOS (Lilly et al. 2007) surveys as well as photometric classification using the long spectral baseline spectral energy distribution (SED) covered in COSMOS (Capak et al. 2007; Salvato et al. 2009; Ilbert et al. 2009a; P. Capak et al. 2009, in preparation). As such, only objects with high-confidence classification enter our sample.

For ∼550 type-1 AGNs selected this way we require the following data, resulting in a random subsample: (1) coverage by ACS F814W (Scoville et al. 2007; Koekemoer et al. 2007), and (2) NICMOS parallels,[15] as well as (3) spectra for virial M_{BH} estimates from the Mg II broad emission line.

The limiting factors are the relative NIC3 coverage of 6.4% of the ACS area (∼20 AGNs) and the status of ongoing spectroscopic surveys. BH masses have been calculated by Trump et al. (2009b) from IMACS spectra and by Merloni et al. (2009) using zCOSMOS/VIMOS. For this Letter, we have BH masses available for 10 AGNs, spanning the redshift range $1 < z < 2$. Two AGNs were observed by both instruments—the M_{BH} estimates are consistent within 0.2 dex in both cases. Sample information is listed in Table 1, including BH masses and galaxy parameters derived below.

3. HOST GALAXY MASSES

3.1. Observed Host Galaxy Photometry and Colors

We obtain information on the host galaxies using broadband photometry from the high-resolution *HST* ACS/WFC images in the F814W ($= I$) filter with $0''.03$/pixel sampling (Koekemoer et al. 2007), and the NICMOS/NIC3 parallels in the F160W ($= H$) filter at $0''.101$/pixel, both integrated for one orbit.

In the NICMOS H band, the host galaxies of all AGNs are clearly resolved, visible already to the unaided eye. We hence extract the host galaxy flux from the composite galaxy+AGN NICMOS image by modeling the two-dimensional light distribution of each object using GALFIT (Peng et al. 2002; C. Y. Peng 2009, in preparation) in Version 3.0 (C. Y. Peng 2009, private communication). We restrict our models to a point source plus a single elliptical Sérsic (1968) profile. Previous simulations show that at our resolution and depth it is unreliable to use many and/or complex galaxy components (Simmons & Urry 2008; Sánchez et al. 2004). We carry out several passes of GALFIT, first with free Sérsic parameter[16] n, and subsequently fixed $n = 1$, 2, or 4, depending on the best free-n fit.

We require GALFIT to converge on a sensible solution, indicating that an actual host galaxy is being described and not, e.g., uncertainties in the point-spread function (PSF). This means we require a GALFIT nucleus-to-host contrast of < 3.25 mag, a half-light radius of $r > 2$ pixel, and $0.5 < n < 8$.

XID 2261 and 5230 both show unrealistically compact host galaxy model scale lengths, indicating an unsuccessful GALFIT model. For these two cases, we simply subtract the best-fitting single point-source model—without a Sérsic component—from the original image, resulting in an only slightly oversubtracted/ underestimated host galaxy. We use aperture photometry on the host galaxy in these cases, and the GALFIT galaxy model magnitude for the other eight.

In total we resolve *all* 10 host galaxies in the sample— no object drops from the sample due to high nucleus-to-host contrast or other reasons. Extracted host galaxy images are shown in Figures 1 and 2.

---

[15] http://irsa.ipac.caltech.edu/data/COSMOS/images/nicmos/

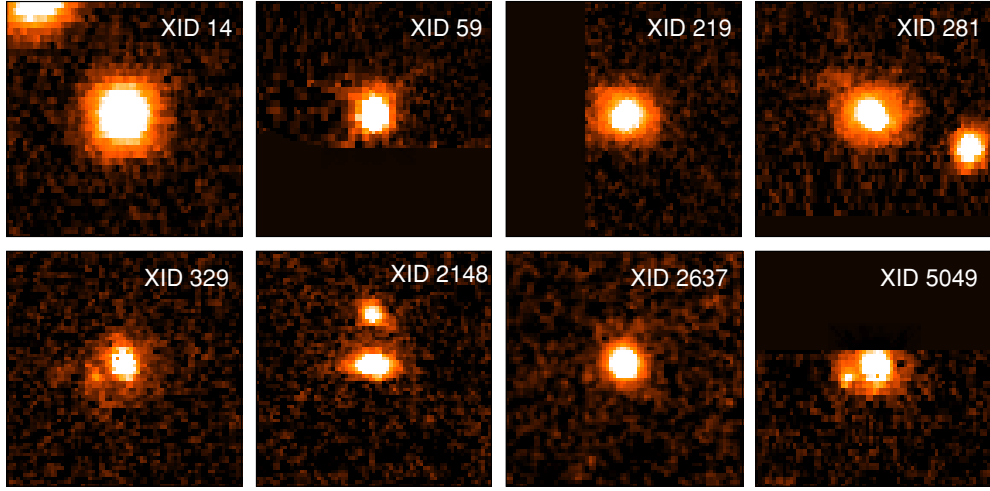[16] $n = 1$ represents an exponential disk; $n = 4$ a de Vaucouleurs spheroid.

Figure 1. Nucleus-removed host galaxies: galaxy plus nucleus model fitted for 8/10 objects (*HST*/NIC3 F160W). Images are $7'' \times 7''$, some objects lie near NICMOS tile edges.
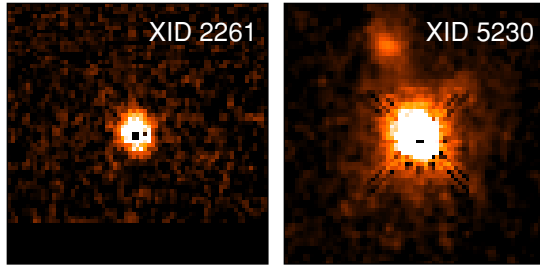

Figure 2. Same as Figure 1: XID 2261 and 5230, only nucleus model fitted and subtracted.

In the ACS *I*-band data, the contrast between AGN and host galaxy is less favorable than in the *H* band, as expected from the near-UV SED. Therefore, we take a two-step approach. First, we carry out "peak subtraction" removal of the nuclear component for the *I* band, by scaling a PSF to the central 4 pixel aperture flux. From statistics on the expected random residuals after subtraction of this scaled PSF for several 1000 stars (Jahnke et al. 2004b), we require a residual flux of >5% for a host galaxy to have a high probability of being resolved. This is the case for 7/10 objects—the hosts of XIDs 59, 2261, and 5230 remain unresolved in the ACS image.

The seven resolved objects are again modeled using GALFIT, with Sérsic *n* fixed from the *H*-band fit, thus minimizing signal-to-noise-ratio-dependent biases in our extracted colors. As for the *H* band, we check the models for successful convergence, which is the case for all seven resolved objects, and again use the host model magnitude. The resulting host galaxy photometry is also listed in Table 1.

3.2. Host Galaxy Stellar Masses

Our general approach is to constrain the mass-to-light ratio (M/L) of each host galaxy by a single optical color. We have successfully employed this method before to study stellar populations of low-*z* quasar host galaxies (Jahnke et al. 2004a) or stellar ages and masses of quasar hosts at $0.5 < z < 3$ (Sánchez et al. 2004; Jahnke et al. 2004b; Kuhlbrodt et al. 2005; Schramm et al. 2008). Here we compute stellar masses from the rest-frame *V*-band luminosity in combination with the M/L

from the rest-frame $(B - V)$ color:

$$L_V = 10^{-0.4(V-4.82)}, \qquad (1)$$

$$M_{*,\text{total}} = 10^{-0.952+1.710(B-V)} \times L_V, \qquad (2)$$

with *L* and *M* in solar units. This calibration is based on template-fitted masses (Bruzual & Charlot 2003, Chabrier IMF) and luminosities derived for galaxies in the COSMOS field (Ilbert et al. 2009b). We convert luminosities to Vega zero-point and apply a -0.124 dex mass offset to transform to the mass scale of the models by S. Charlot & G. Bruzual (2007/2009, in preparation) that include contributions from TP-AGB stars. The linear relation of Equation (2) is a fit to galaxies in redshift-($1.0 < z < 1.6$) and color-range ($0.38 < (B - V) < 0.74$) of our seven host galaxies resolved in both *HST* bands. The scatter of the fit corresponds to an rms uncertainty in resulting stellar mass of ±0.3 dex.

We convert our measured (F814W–F160W) colors to rest-frame $(B - V)_{\text{host}}$ by applying both *K*-correction and a color term, individually for each object and its redshift. For this purpose, we identify for each galaxy the single stellar population model again from Charlot & Bruzual (Chabrier IMF, solar metallicity) with the closest (F814W–F160W) at a given *z*. Since the interpolation intervals are rather small and we are not using the interpolation SED to extract any further information, this method is quite insensitive to the exact choice of models, and errors from M/L calibration dominate.

For the three host galaxies only detected in F160W, we have to make assumptions for the interpolation template to convert observed F160W to L_V, as well as the color (or M/L) in Equation (2). On the red/old side, we assume a value of $(B - V) = 0.75$ (Vega ZP) corresponding to the red end of the red sequence at $z \sim 1.5$ (Kriek et al. 2008), a value also consistent with the reddest values of the rest of the sample. As a blue limit we use $(B - V) = 0.15$, corresponding to 3σ from the mean value for COSMOS inactive galaxies at $z \sim 1.4$, $\log M_{*,\text{total}} > 10.7$ and age $t < 1$ Gyr. These assumptions should bracket the true M/L, and provide robust limits on the host galaxies' stellar mass.

3.3. Stellar Mass Uncertainties

Uncertainties in stellar mass have several sources. In addition to the $(B - V)$ calibration stated above, the strongest contribu-

tions come from (1) GALFIT precision of extracting the host galaxy, (2) potential influence from different spatial resolutions in the ACS and NIC3 images, and (3) dependency of bandpass conversions on assumed templates.

1. Sánchez et al. (2004) tested how reliably GALFIT can derive host galaxy photometry in one-orbit ACS data. Given the typical host galaxy magnitude of our sample in the F814W filter we conclude an uncertainty of 0.15 mag for F814W, and—due to counteracting effects of lower spatial resolution but more favorable galaxy-to-nucleus contrast—also for F160W.

2. GALFIT's functionality depends on the spatial resolution of an image and the spatial difference between the AGN and galaxy component. If a galaxy is compact and the PSF not well characterized, flux transfer between components is possible, its amplitude potentially depending on spatial resolution. We test if the different resolutions of the ACS and NIC3 have a significant influence, by rebinning a mock AGN+galaxy image resembling a typical object to different spatial resolutions. The recovered host galaxy photometry shows an rms variation of ∼0.15 mag, no systematic offset, and a negligible trend with resolution. This rms scatter is consistent with the GALFIT precision from (1) above and we conclude that resolution effects are insignificant.

3. The bandpass conversion and *K*-correction depend on the IMF and metallicity of the assumed single population interpolation model. The masses derived from Chabrier and Salpeter IMF generally differ by less than 0.1 dex. The metallicity of galaxies of the estimated masses at $1 < z < 2$ is expected to range between solar and 3× solar ($8.8 < 12 + \log(O/H) < 9.2$; Tremonti et al. 2004; Maiolino et al. 2008). Changing from the solar metallicity used, to the most metal-rich templates ($Z = 0.05$), masses change by $\lesssim 0.05$ dex. We conclude that our stellar masses should be good to within ∼0.1 dex from the choice of bandpass conversion SEDs.

In combination we find our error budget in stellar mass is 0.21 mag for the $(B - V)$ color (0.15 mag from each band), corresponding to 0.27 dex uncertainty in stellar mass—dominating the three sources of uncertainty above. Adding the uncertainty of the mass calibration from Equation (2), the total uncertainty in stellar mass is ±0.4 dex.

4. RESULTS

While we cannot estimate bulge masses directly, we find that the seven objects with direct *total stellar mass* estimates fall directly onto the M_{BH}–$M_{*,bulge}$ relation (Figure 3) of the local universe from Häring & Rix (2004). The three objects with a bracketing range on stellar mass are also consistent with the local relation. The objects have a maximum deviation of ∼0.3 dex perpendicular to the $z = 0$ relation. The seven non-limit AGNs in the *z*-range $1.06 < z < 1.65$ show a mean ratio $M_{BH}/M_{*,total} = 0.00178 \pm 0.0012$ and mean $\log(M_{BH}) = 8.31$. This is consistent with the value at $z = 0$ of $M_{BH}/M_{*,bulge} = 0.00165$ at the same M_{BH}, and has exactly the same 0.3 dex scatter.

Merloni et al. (2009) compute stellar masses for a larger sample of COSMOS type-1 AGNs, using an independent SED-decomposition method. For 18 galaxies where stellar masses could be estimated with both methods (five objects are part of this study, 13 have no BH mass estimates yet), their masses are smaller by 0.1–0.2 dex. This agreement within the error bars
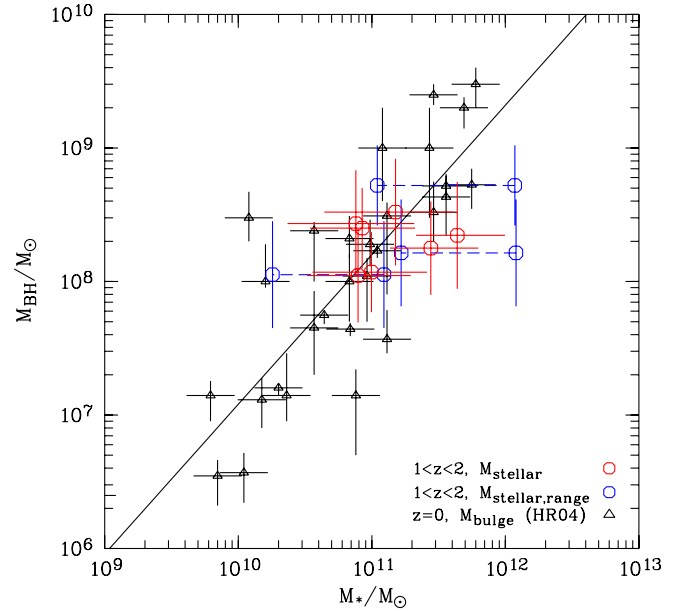

Figure 3. M_{BH}–$M_{*,total}$ relation from COSMOS ACS+NIMOS: shown are 10 type-1 AGNs in the redshift range $1.06 < z < 1.92$, seven with direct stellar mass estimates (red circles) and three with bracketing range (blue circles and lines). The points are overplotted over the local M_{BH}–$M_{*,bulge}$ relation by Häring & Rix (2004) (black triangles) and its best fit (solid line, $\log M_{BH} = 8.2 + 1.12 \times (\log M_{*,bulge} - 11)$). At a given mass, there is no difference in the $M_{BH}/M_{*,total}$ ratio at $z \sim 1.4$ and local $M_{BH}/M_{*,bulge}$ ratio, for the sampled BH mass range, $\log M_{BH} \sim 8.3$.

reinforces our conclusion that our mass estimates are robust. In total they find a mild deviation from the $z = 0$ relation, but most of their signal comes from objects at $z > 1.5$, which is not well covered by our study.

5. DISCUSSION AND CONCLUSIONS

5.1. Completeness and Systematics

Are there systematic effects inherent in the data set that prevent us from detecting objects that deviate more strongly from this relation? X-ray selection and subsequent broad-line AGN classification find all AGNs down to a contrast of AGN/galaxy $\lesssim 10\%$, beyond which the stellar light swamps any AGN signature. The general limit is set by the magnitude limit of the spectral follow up, modified by this contrast. At the observed M_{BH} we expect generally high accretion rates (e.g., Zheng et al. 2009), thus this detection limit converts to a limit in M_{BH} present in the data. The additional ACS and NIC3 coverage are random processes. Being able to extract a host galaxy for every single object of our sample means that aside from the M_{BH} limit we have no completeness limitations with respect to galaxy mass. In summary, we do not expect missing objects in the M_{BH} regime currently populated.

We also comment on the luminosity function or "Lauer" bias (Lauer et al. 2007): the M_{BH}–$M_{*,total}$ relation has a scatter and the BH luminosity function drops rapidly toward higher *L*. In combination, a flux-limited sample of AGN will select many more massive BHs in lower mass galaxies than vice versa, biasing the sample toward higher M_{BH}.

Despite the local comparison sample not being selected by M_{BH}—it consists of inactive galaxies—we do not expect a large bias: the Merloni et al. (2009) and Trump et al. (2009b) BH masses follow the mass calibration by Onken et al. (2004). Their virial M_{BH} for active galaxies are calibrated by a forced

match to the $M_{\rm BH}$–σ_* relation for inactive galaxies. This might create "wrong" $M_{\rm BH}$ estimates, but it compensates most of the expected offset $\Delta M_{\rm BH}$ between our AGN sample and any (active or inactive) sample in the local universe. Together with only a small scatter in the local $M_{\rm BH}$–$M_{*,\rm bulge}$, it is not surprising to find no discernable signature of the LF bias in our data.

5.2. For Massive Galaxies: Relative Non-Evolution of BH Mass Versus Total Stellar Mass

Häring & Rix (2004) derive dynamical *bulge* masses—we derive *total* stellar masses of the host galaxies. Interpreting the coincidence of these two relations at $z = 0$ and $z \sim 1.4$ depends on how much stellar mass in our sample is actually part of a disk component. The stellar masses of $\log M_{*,\rm total} = 11.1 \pm 0.3$ are already high in the galaxy mass function and our sample galaxies are the likely progenitors of giant ellipticals in the local universe. If they were already bulge-dominated at the observed redshifts, nine billion years earlier, our total masses revert to bulge masses and our observations mean zero evolution (though consistent with evolution of factor <2.65 within errors) in $M_{\rm BH}$–$M_{*,\rm bulge}$, at these $M_{\rm BH}$.

5.3. Evolution of BH Mass Versus Bulge Mass and Velocity Dispersion

While the actual bulge-to-total mass ratio $(B/T)_{\rm mass}$ of our galaxies—in fact of any galaxy at these redshifts—is unknown, we have circumstantial evidence that our galaxies could contain substantial disk components: (i) visual impression in Figures 1 and 2, (ii) some galaxies have Sérsic indices near $n = 1$ (Table 1), (iii) some best-fitting SSP models have ages down to 1 Gyr (oldest: 5 Gyr), (iv) the $z = 0.36$ host galaxies of Treu et al. (2007), with similar $M_{\rm BH}$, have $(B/T)_{\rm mass} \sim 1/3$, (v) more than 50% of $\log M_{*,\rm total} = 11.1 \pm 0.3$ galaxies are strongly star forming at $z \sim 1$ (Noeske et al. 2007), and (vi) of them $\lesssim 40\%$ are on the red sequence (at $z = 1.5$; Taylor et al. 2009).

With a substantial disk component a different interpretation is possible.

1. We know, independently of their exact evolutionary path, these galaxies have to end up on the local $M_{\rm BH}$–$M_{*,\rm bulge}$ relation. If they currently obey the same relation but with $M_{*,\rm total}$, then their masses in bulge+disk at $z = 1.4$ can end up in their bulges 9 Gyr later with no addition of mass to either the BH or the bulge from outside the galaxy or from star formation.

2. What is required is a process redistributing disk stars to the bulge: major and minor galaxy merging (Hopkins et al. 2009) and disk instabilities (Parry et al. 2009) together dominate bulge-creation at high masses.

3. In addition to the disk-to-bulge conversion process these galaxies can still grow. Merging of similar systems will just coadd BHs and stellar components separately, moving the system parallel along the local scaling relation. However, total mass growth is limited since the observed evolution in space density of massive galaxies at $z < 1.5$ is small (e.g., Ilbert et al. 2009a, and references therein).

4. Even wet mergers are allowed: the gas conversion efficiency is not very high—in individual mergers (Croton 2006) and also overall (at $z \sim 0.6$; Robaina et al. 2009) only 10% of the SF arise from merging.

5. Any subsequent (or ongoing) AGN phase will also less than double the BH mass, since high accretion states are rare and short (Hopkins et al. 2006). Any BH or stellar mass change

below a factor of 2 will lie within the 0.3 dex scatter of the local relation.

In the case of a disk component in our galaxies at $z = 1.4$, bulge masses are smaller than the total stellar mass in Figure 3 and the $M_{\rm BH}$–$M_{*,\rm bulge}$ relation will actually evolve, when the galaxy structures are changing over time through merging. They will constantly move closer to the local relation—consistent with predictions from simulations of a merger-driven bulge evolution (Croton 2006).

This has the implication that our result is consistent with the non-evolution of the *bulge* mass relation at $z < 1.7$ for massive early-type quasar host galaxies found by Peng et al. (2006a, 2006b)—there $M_{*,\rm bulge} = M_{*,\rm total}$. At the same time, we agree with the strong evolution in $M_{\rm BH}$–$M_{*,\rm bulge}$ and $M_{\rm BH}$–$\sigma_{*,\rm bulge}$ claimed by Treu et al. (2007) and Woo et al. (2008): if we assume as a limit for our galaxies $(B/T)_{\rm mass} \leqslant 1/3$, our results predict an evolution of $M_{\rm BH}/M_{*,\rm bulge} \leqslant (1+z)^{1.2}$, consistent with $M_{\rm BH}/M_{*,\rm bulge} \leqslant (1+z)^{1.5\pm1.0}$ found by Treu et al. (2007) for Seyfert 1 galaxies of the same BH mass at $z = 0.36$.

This path of converging co-evolution of bulge and BH is fully independent of any interaction or feedback *between* bulge and BH—the AGN can even be switched off since $z = 1.4$. What we are witnessing is the formation of the bulge independent of the BH. Only before $z = 1.4$ is a mechanism required to connect total stellar mass and BH mass in massive galaxies. We might see an indication of this in the large offset of the relation for $z > 4$ (Walter et al. 2004; Riechers et al. 2008a, 2008b, 2009), but the Lauer-bias and the different mass scale ($M_{\rm BH} > 9.2$) complicate the picture. Since stellar mass and BH mass buildup trace each other very well over cosmic time with a factor similar to the local ratio of BH and stellar mass (Zheng et al. 2009), the coupling mechanism can be very indirect and does not need to be dominated by a strong version of AGN feedback.

REFERENCES

Brusa, M., et al. 2007, ApJS, 172, 353
Bruzual, G., & Charlot, S. 2003, MNRAS, 344, 1000
Capak, P., et al. 2007, ApJS, 172, 99
Cappelluti, N., et al. 2009, A&A, 497, 635
Croton, D. J. 2006, MNRAS, 369, 1808
Häring, N., & Rix, H.-W. 2004, ApJ, 604, L89
Hasinger, G., et al. 2007, ApJS, 172, 29
Hopkins, P. F., Hernquist, L., Cox, T. J., Di Matteo, T., Robertson, B., & Springel, V. 2006, ApJS, 163, 1
Hopkins, P. F., et al. 2009, MNRAS, submitted (arXiv:0906.5357)
Ilbert, O., et al. 2009a, ApJ, 690, 1236
Ilbert, O., et al. 2009b, ApJ, submitted (arXiv:0903.0102)
Jahnke, K., Kuhlbrodt, B., & Wisotzki, L. 2004a, MNRAS, 352, 399
Jahnke, K., et al. 2004b, ApJ, 614, 568
Koekemoer, A. M., et al. 2007, ApJS, 172, 196
Kriek, M., van der Wel, A., van Dokkum, P. G., Franx, M., & Illingworth, G. D. 2008, ApJ, 682, 896
Kuhlbrodt, B., Örndahl, E., Wisotzki, L., & Jahnke, K. 2005, A&A, 439, 497
Lauer, T. R., Tremaine, S., Richstone, D., & Faber, S. M. 2007, ApJ, 670, 249
Lilly, S. J., et al. 2007, ApJS, 172, 70
Maiolino, R., et al. 2008, A&A, 488, 463

Marconi, A., & Hunt, L. K. 2003, ApJ, 589, L21
Menci, N., Fiore, F., Puccetti, S., & Cavaliere, A. 2008, ApJ, 686, 219
Merloni, A., et al. 2009, ApJ, in press (arXiv:0910.4970)
Noeske, K. G., et al. 2007, ApJ, 660, L47
Onken, C. A., Ferrarese, L., Merritt, D., Peterson, B. M., Pogge, R. W., Vestergaard, M., & Wandel, A. 2004, ApJ, 615, 645
Parry, O. H., Eke, V. R., & Frenk, C. S. 2009, MNRAS, 396, 1972
Peng, C. Y., Ho, L. C., Impey, C. D., & Rix, H.-W. 2002, AJ, 124, 266
Peng, C. Y., Impey, C. D., Ho, L. C., Barton, E. J., & Rix, H.-W. 2006a, ApJ, 640, 114
Peng, C. Y., Impey, C. D., Rix, H.-W., Kochanek, C. S., Keeton, C. R., Falco, E. E., Lehár, J., & McLeod, B. A. 2006b, ApJ, 649, 616
Riechers, D. A., Walter, F., Brewer, B. J., Carilli, C. L., Lewis, G. F., Bertoldi, F., & Cox, P. 2008a, ApJ, 686, 851
Riechers, D. A., Walter, F., Carilli, C. L., Bertoldi, F., & Momjian, E. 2008b, ApJ, 686, L9
Riechers, D. A., Walter, F., Carilli, C. L., & Lewis, G. F. 2009, ApJ, 690, 463
Robaina, A. R., et al. 2009, ApJ, 704, 324

Salvato, M., et al. 2009, ApJ, 690, 1250
Sánchez, S. F., et al. 2004, ApJ, 614, 586
Schramm, M., Wisotzki, L., & Jahnke, K. 2008, A&A, 478, 311
Scoville, N., et al. 2007, ApJS, 172, 38
Sérsic, J. 1968, Atlas de Galaxias Australes, Observatorio Astronomico de Cordoba
Simmons, B. D., & Urry, C. M. 2008, ApJ, 683, 644
Somerville, R. S., Hopkins, P. F., Cox, T. J., Robertson, B. E., & Hernquist, L. 2008, MNRAS, 391, 481
Taylor, E. N., et al. 2009, ApJ, 694, 1171
Tremonti, C. A., et al. 2004, ApJ, 613, 898
Treu, T., Woo, J.-H., Malkan, M. A., & Blandford, R. D. 2007, ApJ, 667, 117
Trump, J. R., et al. 2009a, ApJ, 696, 1195
Trump, J. R., et al. 2009b, ApJ, 700, 49
Walter, F., Carilli, C., Bertoldi, F., Menten, K., Cox, P., Lo, K. Y., Fan, X., & Strauss, M. A. 2004, ApJ, 615, L17
Woo, J.-H., Treu, T., Malkan, M. A., & Blandford, R. D. 2008, ApJ, 681, 925
Zheng, X. Z., et al. 2009, ApJ, in press (arXiv:0911.0005)